Using RON Synergistic Effects to Formulate Fuels for Better Fuel Economy and Lower CO2 Emissions

Roland Dauphin, Jerome Obiols, David Serrano, Yann Fenard, A. Comandini,
Laurie Starck, Guillaume Vanhove, Nabiha Chaumeix

HAL Id: hal-02413469

https://hal.science/hal-02413469

Submitted on 16 Sep 2020

Using RON Synergistic Effects to Formulate Fuels for Better Fuel Economy and Lower CO2 Emissions

Roland Dauphin, Jerome Obiols
TOTAL Marketing & Services

David Serrano[1], Yann Fenard[2], Andrea Comandini[3], Laurie Starck[1], Guillaume Vanhove[2], Nabiha Chaumeix[3]
[1]IFP Energies nouvelles, [2]Université de Lille, Sc. et Technologie, [3]ICARE-CNRS, INSIS

ABSTRACT

The knock resistance of gasoline is a key factor to decrease the specific fuel consumption and CO_2 emissions of modern turbocharged spark ignition engines. For this purpose, high RON and octane sensitivity (S) are needed.

This study shows a relevant synergistic effect on RON and S when formulating a fuel with isooctane, cyclopentane and aromatics, the mixtures reaching RON levels well beyond the ones of individual components. The same is observed when measuring their knock resistance on a boosted single cylinder engine.

The mixtures were also characterized on a rapid compression machine at 700 K and 850 K, a shock tube at 1000 K, an instrumented and an adapted CFR engine. The components responsible for the synergistic effects are thus identified. Furthermore, the correlations plotted between these experiments results disclose our current understanding on the origin of these synergistic effects.

This study concludes that this synergistic effect encourages formulating highly paraffinic fuels for lower specific fuel consumptions and CO_2 emissions. Thus, paraffins are still relevant compounds to formulate highly efficient gasolines, despite their low octane sensitivity when individually considered. Furthermore, the CFR engine is still the best known device to anticipate synergistic effects in gasoline's knock resistance, through the Octane Index (OI = RON – K.S). A sensitivity study on the "K value" of the octane index shows that octane sensitivity mainly drives the gasoline performance for the low-sensitivity fuels while RON also drives it for the high-sensitivity ones.

INTRODUCTION

Decreasing specific fuel consumptions and CO_2 emissions of passenger cars are major stakes. For instance in Europe, under the European Commission current proposal, average new-vehicle CO_2 emission levels would have to fall by 15% by 2025 and 30% by 2030 in a Worldwide Harmonized Light Vehicles Test Procedure (WLTP) compared to a 2021 baseline. The 2021 baseline being set at 95 gCO_2/km in a New European Driving Cycle (NEDC) after having been set – and successfully met – at 130 gCO_2/km in 2015 [1]. Many countries in the world, including China and the Unites States, follow the same stringent regulation trend [2].

It is well known in the engine community that, as far as spark-ignition engine fuels are concerned, a high knock resistance is required to ensure a high engine effective efficiency (η_{eff}) [3], whose definition is shown in equation (1). Indeed, this particular fuel's quality allows increasing the engine compression ratio, which leads to a higher theoretical thermodynamic efficiency ($\eta_{th.th}$); additionally, it avoids delayed knock-limited combustions, which leads to improved cycle efficiency (η_{cycle}) [4]:

$$\eta_{eff} = \eta_{comb} \times \eta_{th.th} \times \eta_{cycle} \times \eta_{mech} \qquad (1)$$

However, this fuel's knock resistance quality is not sufficient to ensure low specific consumptions (BSFC, expressed in g/kW.h) and low specific CO_2 emissions ($BSCO_2$, in gCO_2/kW.h). For this purpose, as shown in equations (2) and (3) below, the gasoline also must have a high lower heating value (LHV, expressed in MJ/kg) for improved BSFC and a low carbon intensity (CI, in gCO_2/MJ) for decreased specific CO_2 emissions.

$$BSFC = \frac{1}{LHV.\eta_{eff}} \qquad (2)$$

$$BSCO_2 = CI.\frac{3.6}{\eta_{eff}} \qquad (3)$$

The tests results disclosed here were obtained in the frame of the development of racing fuels. This explains why the equivalence ratio used in the tests differs from the usual $\Phi = 1$ (stoichiometry) and is slightly lean instead ($\Phi = 0.85$). The use of lean mixtures in racing engines is encouraged by some racing regulations which stipulate that the fuel flow rate (Q_{fuel}, in g/h) is capped at a maximum value [5]. In this context, as shown in the equation (4), obtaining more engine power (P_{eff}, in kW) requires solely decreasing BSFC, which in the end leads to increasing the fuel's LHV and the engine efficiency. Thus, using lean mixtures is a way, among many others used by racing engines, to increase the engine efficiency through the theoretical thermodynamic efficiency [4]. Finally, the racing engines targets are very similar to the commercial ones which also aim at lower BSFC and increased efficiency. Moreover, the racing engines work at very high load, which is more and more the case of the downsized turbocharged SI commercial engines currently benefiting from a dramatic increase in specific power [6]. Besides, the similarity between the fuel racing regulation and the European regulation for commercial gasoline (EN228) makes the insight learnt during racing fuel developments easily transferable to commercial gasoline for highly efficient engines.

$$P_{eff} = \frac{Q_{fuel}}{BSFC} \qquad (4)$$

Formulating a fuel is a complex process consisting in optimizing the blend of several compounds to reach several targets which are often contradictory. It requires the knowledge of numerous blending laws for each of the compounds in each of the fuel's properties. Concerning octane rating, and more particularly RON, blending laws have been widely studied and regularly show non-linear behaviors [7, 8, 9]. Most of time, the blending laws remain monotonous, which means that the RON of the mixture lies still between the RON of the pure compounds (mathematically speaking, the blending laws remain a bijective function). More rarely, some synergistic effects have been demonstrated. In this study, "synergistic effect" means that the RON of the mixture can be greater than the RON of each of its compounds (or mathematically speaking, the blending law is a surjective function which has at least one derivative equal to zero). For example, Bradow et al. [10] have shown that a mixture of isooctane and diisobutylene (DIB) can reach RON levels greater than the ones of pure isooctane and DIB. Later, Foong et al. [11] have demonstrated another synergistic effect between isooctane and ethanol. These synergistic effects are obviously interesting for formulating a fuel, and consequently, one always targets to benefit from them. Thus, in this study will be demonstrated synergistic effects between isooctane and other compounds.

Isoparaffins, such as issooctane, are interesting compounds for fuel formulation: they have a high LHV

and a low carbon intensity compared to other hydrocarbon families (Figure 1), and they can have a high RON provided that their structure is well selected [12]. Although their octane sensitivity varies widely (from -18.9 to 12.5 according to [13]), they are often too simply considered as low octane sensitivity components. This can lead to the flawed conclusion that, as long as a high octane sensitivity is desired for fuel performance, their incorporation is detrimental. Boot et al. [14] have indeed demonstrated that, from a statistical point of view, a higher paraffinic fraction leads to lower octane sensitivity, which leads to a lower Octane Index in modern turbocharged engines, which in the end leads to a lower fuel performance [15, 16, 17, 18]. But the use of optimized blending laws, such as those described above, allowing to create synergistic effects with isoparaffins on RON and octane sensitivity, could radically change this conclusion. In this case, increasing the fraction of isoparaffins could even boost the fuels performance under certain conditions. This is the focus proposed by this study.
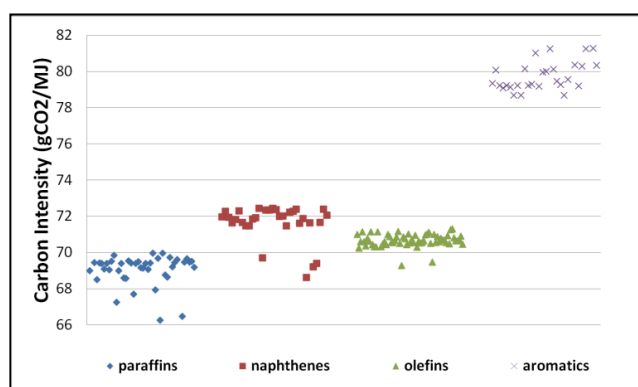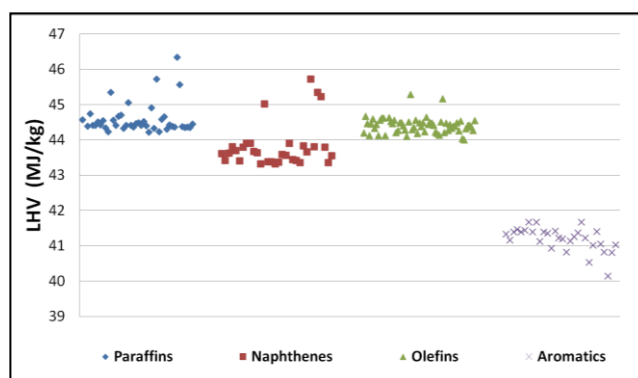

Figure 1: Lower Heating Values (top) and Carbon Intensities (bottom) of compounds in each hydrocarbons family. Raw data from [13], calculations by the authors.

Finally, once the synergistic effects on RON are observed, several questions may be raised:

- First, are those effects due to a "bias" induced by the CFR method in which the equivalence ratio is not fixed; or are they due to a "real" effect induced by the chemistry of the mixture? Adapted tests achieved on an instrumented CFR engine will allow answering this first question.

- Then, is it possible to reproduce these synergistic effects on more fundamental

experimental devices, to understand their origin? Lu et al. [19] have led experiments in a flow reactor and have concluded that the synergistic effect between isooctane and ethanol on RON may be due to ethanol's capacity to consume OH radicals at low temperature. In the present study, no flow reactor was used, but ignition delay times have been measured at low (700 K), intermediate (850 K) and high (1000 K) temperatures on a rapid compression machine and a shock tube instead. These experiments measuring ignition delay times aim at trying to reproduce this synergistic phenomenon on these devices, and therefore provide some insight.

- Furthermore, do these synergistic effects observed on the CFR engine create "real" benefits in terms of knock resistance in a modern turbocharged engine? If so, how do they translate into specific fuel consumption and CO_2 emissions benefits? Engine tests achieved in the frame of this study will allow assessing those benefits.

- Finally, for a given fuel, which fuel properties should be enhanced in priority to improve the engine's performance? Studying the evolution of the K value in the Octane Index (OI = RON – K.S) allows answering this question: if K is lower than -1, it means that the Octane Index is better improved by increasing the octane sensitivity than the RON; on the contrary, if K is greater than -1, increasing the RON improves the Octane Index better than increasing the octane sensitivity. It has been well demonstrated that the K value varies with the engine operating point [15, 17, 18, 20]: it generally reaches a minimum value for the low engine speeds and high loads operating points (low-end torque area), and increases when reducing the load or increasing the engine speed. The present study focuses on the variations of K depending on the fuel's octane sensitivity: thanks to the engine evaluation of a large number of fuels having various octane sensitivities, it will be shown that there exists a threshold of octane sensitivity under which increasing the octane sensitivity matters more than increasing the RON for the sake of engine performance; above this threshold, RON and octane sensitivity are shown to be equally important to the engine performance.

FUEL MATRIXES

The work presented in this paper aims at studying the synergistic effects between two fuels: "A" and "B". Fuel A is a mixture of 75% w/w of cyclopentane (97% purity) and 25% w/w of various aromatic compounds (99% purity), while Fuel B is principally composed of isooctane (2,2,4-trimethylpentane, 95% purity). The main characteristics of Fuel A and B are given in Table 1. It can be observed a bigger lower heating value (LHV) for Fuel B than for Fuel A, due to the paraffinic nature of fuel B compared to the naphthenic and aromatic content of Fuel A. Fuel B's C/H ratio is also lower than Fuel A's for the same reason. Furthermore, Fuel B's RON and MON were measured at 100, in accordance with the scale of RON and MON defined on isooctane. Consequently, Fuel B has an octane sensitivity of 0, while Fuel A, composed of octane sensitive components, has an octane sensitivity equal to 17.5, with a RON of 103.1 and a MON of 85.6.

Fuel		Fuel A	Fuel B
Cyclopentane	% w/w	75	0
Aromatics	% w/w	25	0
Isooctane	% w/w	0	100
LHV	kJ/kg	43 070	44 292
C/H ratio	w/w	6.579	5.295
AFR st.	w/w	14.51	15.13
RON	-	103.1	100
MON	-	85.6	100
Sensitivity	-	17.5	0

Table 1: Main physical-chemical characteristics of Fuels A and B.

To study the synergistic effects between Fuel A and B, the two fuels were blended in different proportions. These mixtures were characterized on a rapid compression machine (RCM, at 700 K and 850 K), a shock tube (ST, at 1000 K), a CFR engine using the standard methods (RON and MON), a CFR engine using fixed equivalence ratios (RON-Φ) and a single cylinder engine (SC). Each mixture is called A-x/B-y, with x and y being the respective ratio (in % w/w) of Fuel A and B composing the blend. These mixtures are gathered in Table 2, and the corresponding experiments that were achieved are cross-marked. In short, all mixtures were characterized using all experimental methods, except Fuel A-10/B-90 which was not tested on the single cylinder engine.

As will be discussed later on, a synergistic effect exists between Fuel A and B. As one of the goals of this study is to understand the origin of this synergy, Fuel A was split in 2 parts: Fuel A1, made solely of cyclopentane, and Fuel A2, only composed of aromatics. Then, mixtures of Fuel A1 and B, as well as mixtures of Fuel A2 and B were evaluated on a CFR engine as shown in Table 3.

Fuel	A-100/B-0	A-85/B-15	A-69/B-31	A-50/B-50	A-30/B-70	A-10/B-90	A-0/ B-100
A (% w/w)	100	85	69	50	30	10	0
B (% w/w)	0	15	31	50	70	90	100
Cyclopentane (%w/w)	75	62	50	36	22	8	0
Aromatics (% w/w)	25	23	19	14	8	2	0
Isooctane (% w/w)	0	15	31	50	70	90	100
RCM, 700 K	X	X	X	X	X	X	X
RCM, 850 K	X	X	X	X	X	X	X
ST, 1000 K	X	X	X	X	X	X	X
RON	X	X	X	X	X	X	X
MON	X	X	X	X	X	X	X
RON-Φ	X	X	X	X	X	X	X
SC	X	X	X	X	X		X

Table 2: Fuel mixtures based on Fuel A and B: compositions and relevant experiments (cross-marked)

Fuel	A1-100/ B-0	A1-75/ B-25	A1-50/ B-50	A1-25/ B-75		A2-100/ B-0	A2-75/ B-25	A2-50/ B-50	A2-25/ B-75
A1 (% w/w)	100	75	50	25		0	0	0	0
A2 (% w/w)	0	0	0	0		100	75	50	25
B (% w/w)	0	25	50	75		0	25	50	75
Cyclopentane (%w/w)	100	75	50	25		0	0	0	0
Aromatics (% w/w)	0	0	0	0		100	75	50	25
Isooctane (% w/w)	0	25	50	75		0	25	50	75
RON	X	X	X	X		X	X	X	X

Table 3: Fuel mixtures based on Fuel A1 and B (left) and based on Fuel A2 and B (right): compositions and relevant experiments (cross-marked).

EXPERIMENTAL METHODS

In this section are briefly described the different experimental methods used in this study to characterize the ignition delay times at three different levels of temperature. The octane rating method is also described, both using the standard CFR method and a specifically designed method for evaluating octane numbers at constant equivalence ratio. Finally, the single cylinder engine on which the fuels have been evaluated is also described in this section, along with the test method to characterize them.

IGNITION DELAY TIMES

Rapid Compression Machine

Ignition delays were measured in the U.Lille Rapid Compression Machine (RCM), which consists of two pistons: a pneumatically driven piston and a compressing piston, both connected by a moving cam, following a right-angle design. This ensures a highly reproducible compression phase as well as a strictly constant volume after compression. While the operating procedure of this apparatus have been described extensively in the literature [21, 22], a brief description of the hereby reported experiments will be given here. The compression time was fixed at 60 ms, and monitored with help from an optocoupler. Mixtures of the fuel blends described in the "Fuel Matrix" section and synthetic 'air' were prepared in a heated mixture preparation facility at a fixed temperature of 80°C, following the partial pressure method. The injection of the fuel mixture was performed using a liquid syringe, ensuring total evaporation of the injected fuel inside the facility. In order to reach target compressed temperatures of 700 and 850 K, Nitrogen (N_2) and Argon (Ar) were used respectively as the inert gas. High purity (>99.99%) oxygen, Nitrogen and Argon were provided by Air Liquide. The mixtures were transferred to the RCM through a gas line heated to 80°C, the reaction chamber temperature being adjusted to reach the target temperatures precisely. Special attention was dedicated to ensuring that the temperature was sufficient so the vapor pressure of the fuel components exceeded their partial pressure by a factor of two at all times. Compressed gas temperatures T_C were calculated from the initial composition, pressure, temperature and from the compressed pressure using the adiabatic core assumption. The pressure was measured throughout the experiment by a thermal-shock protected piezoelectric pressure transducer Kistler 6052 connected to a 5017 charge amplifier. The first-stage and total ignition delays are defined as the time between the maximum of pressure corresponding to the end of compression and the maximum of the derivative of pressure corresponding to the first-stage ignition, and total ignition respectively. All experiments were performed a minimum of three times to ensure the reproducibility of the measurements.

Additional analyses of the pressure traces were carried out to evaluate the chemical heat release induced by the first-stage ignition, using the following application of the first principle of thermodynamics to calculate the heat release rate (HRR):

$$HRR = \frac{\gamma}{\gamma-1} \cdot p \cdot \frac{dV}{dt} + \frac{1}{\gamma-1} \cdot V \cdot \frac{dp}{dt} \qquad (5)$$

The evolution of the reactive volume was deduced from unreactive experiments, where the oxygen in the mixture was replaced by nitrogen. The accumulated heat release was computed by integrating HRR from the time at top dead center onwards. It should be noted that such a calculation is only qualitative, and will not account for increased heat loss, mass transfer to the crevice and modification of the composition of the mixture during the first-stage ignition event [23]. As a consequence, this analysis will only be performed to compare different fuel blends in the same compressed conditions, and no absolute values of the accumulated chemical heat release are reported here.

Shock Tube

In order to extend the study to higher temperatures, ignition delay times were measured in the High temperature high pressure shock tube at ICARE-CNRS laboratory (HTHP-ST). It consists of a stainless tube with a total length of 7.15 m. The high pressure section (2 m long and 114 mm i.d.) is connected to the driven section (5.15 m long and 52 mm i.d.) through a double diaphragm section. The inner walls of the shock tube are mirror-polished in order to reduce the wall rugosity. The shock wave is produced by the sudden burst of a couple of diaphragms mounted between the driver and the driven side of the shock tube. The last two sections (1.4 m long) were blackened with a special surface treatment in order to suppress multiple reflection of light near the measurement section. The last section (0.7 m long) is equipped with four piezo-electric shock detectors (CHIMIE METAL, A25L05B) flush-mounted with the internal surface of the shock tube. They are equally spaced (150 mm), the last one being 15 mm before the end wall of the shock tube. At the same position as the last shock detector, a PCB pressure transducer and two quartz windows (8mm optical diameter) are mounted. Finally a Kistler (603B) pressure transducer is mounted at the end-wall (reflecting surface) of the shock tube in order to monitor the pressure during the observation time. The pressure profiles from four CHIMIE METAL A25L05B sensors provided the measurement of the incident shock wave velocities. They were subsequently used together with the initial conditions to calculate the pressure and temperature conditions behind the reflected shock waves by solving the conservation equations. The method used for the calculations assumes thermal equilibrium and no reaction before ignition as well as variable γ. The estimated errors in the temperature and pressure calculations are respectively 1% and 1.5% [24, 25]. Since the studied mixtures are non-diluted and since the ignition delay times (which are the targets) are around or exceed the millisecond, it is necessary to compensate for the non-ideal behavior of the shock tube. For that purpose, inserts in the driver section were used to ensure that the pressure remains approximately constant during

the ignition delay time, and make sure that any increase in pressure is due to the reaction and not to the non-idealities of the shock tube as can be seen in Figure 2.
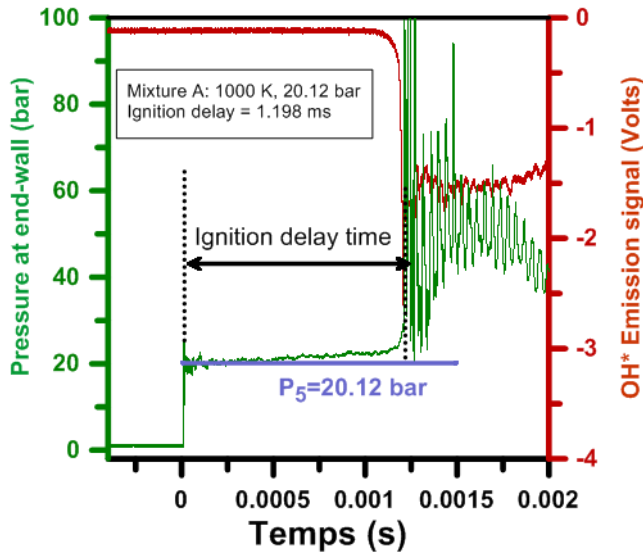

Figure 2: Pressure profile and OH* emission profile measured in the shock tube at ICARE-CNRS laboratory for Fuel A. The conditions behind the reflected shock wave are 20.12 bar and 1000 K.

In addition, spectrophotometric measurements were performed for both the CH* and the OH* radicals. In the present work, the ignition delay time can be defined as the time between the arrival of the incident shock wave at the end-wall and (i) the time when the OH* profile reaches the 50% of its maximum value, or (ii) the slope of the steep pressure increase. Since these mixtures are non-diluted, both methods give the same value. Uncertainty in the ignition delay time measurement does not exceed 5 %.

OCTANE RATING

The Octane Number (ON) measurements were carried out on the standardized CFR engine at IFP Energies nouvelles (IFPEN). The CFR engine is a model F-1/F-2 engine equipped with a CFR-48 crankcase type. It is a two valve four-stroke single-cylinder spark-ignition engine (see Table 4 for main engine specifications) with specific features that allow varying the Compression Ratio (CR) from 4.5:1 to 18:1 by moving the cylinder height. The engine is connected to an electric synchronous motor that maintains a constant rotational speed both in fired and motored conditions.

Bore x Stroke	82.55 x 114.30 mm
Cylinder displacement	611 cm^3
Compression Ratio	4.5:1 to 18:1

Table 4: CFR engine main geometrical features.

The CFR engine is equipped with a four-bowl variable-level carburetor supplying the fuel to the engine. This configuration allows a fast alternation between the tested fuel and the two reference PRFs (Primary Reference Fuel) without stopping the engine, as required in the ASTM Standard procedure [26].

The knock intensity is evaluated by means of a detonation pickup (Figure 3). This sensor is a magnetostrictive type transducer that threads into the engine cylinder and is exposed to combustion chamber pressure in order to provide an electrical signal that is proportional to the rate of change of cylinder pressure. This signal is finally displayed on the Knockmeter which shows the knock intensity (which ranges between 0 and 100) and is later referred as KI. The standard level of KI is defined at 50. Two controls are available to calibrate this knock measuring chain: the *spread* which is the gain or sensitivity (KI divisions per ON) and the *meter reading* which is the offset as described in Figure 3.
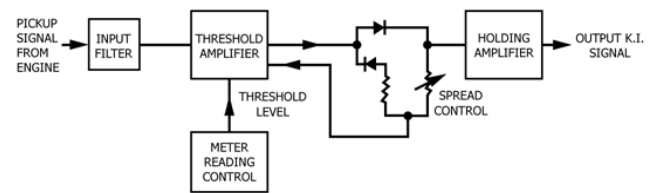

Figure 3: Block Diagram of Knock Measurement System from D2699 ASTM procedure [26].

Besides, for this specific study, a NGK UEGO sensor was mounted on the exhaust line of the CFR engine. This sensor measures the equivalence ratio evolution (referenced as Φ). This sensor will be useful for the octane rating at constant equivalence ratio.

In this study, two methods were used to measure RON: the standard method, and an adapted method at constant equivalence ratio. For the sake of clarity, the two paragraphs below are dedicated to the description of each method, the goal being to better understand the differences in the process of measurement, and consequently the differences on the results given by each method.

Standard RON, MON and Octane Sensitivity measurements

The standard ASTM D2699 (EN-ISO 5163) [26] and ASTM D2700 (EN-ISO 5164) [27] describe the procedures for assessing the RON and MON respectively.

Parameter	RON Research Octane Number	MON Motor Octane Number
Engine speed	600rpm	900rpm
Spark timing	13CAD	variable
Intake air temperature	28.3°C	38°C
Fuel carbureted mixture	Ambient	149°C

Table 5: CFR main operating conditions for RON and MON.

The principle of a RON standard measurement is to run the CFR engine at 600 rpm, with a controlled air mixture and temperature as shown in Table 5. The

objective is to compare the knock characteristics of a sample fuel with those of 2 PRF blends for which the ON is known. The engine parameters that are adjusted are the CR and equivalence ratio. The latter is varied to maximize the KI as shown in Figure 4. For the knock measurement, the spread and the meter reading need to be calibrated.
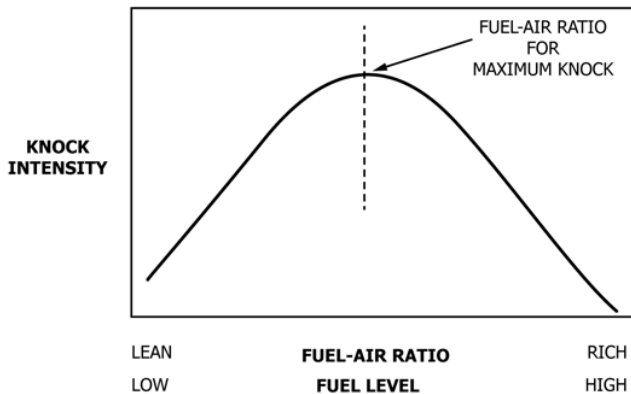

Figure 4: Typical Effect of Fuel-Air Ratio on Knock Intensity [26].

The standard RON procedure is quite complex and long but it is useful to summarize its main steps:

STEP 1 - CFR engine standardization: the CFR engine is calibrated using a standardized fuel (tri-component toluene-isooctane-heptane fuel) to operate at standard KI (50).

STEP 2 - First RON evaluation for the sample fuel: the equivalence ratio of the sample fuel is varied to maximize the KI, and then the engine CR is adjusted so that the standard KI (50) is achieved. Then the standard KI guide table relates the CR of the engine to a first RON value for the sample fuel.

STEP 3 - Selection of PRF and calibration of knock measurement chain: Without changing the CR, two PRF blends are selected (PRF1 and PRF2) so that, at their equivalence ratio for the maximum KI, one knocks more (higher KI) and the other less (lower KI) than the sample fuel. The knock measurement chain is calibrated by adjusting the meter reading and the spread with the two PRFs. Both calibration settings will remain unchanged for the rest of the procedure.

STEP 4 - sample fuel's RON determination: the CR is adjusted to obtain the standard KI (50) for the sample fuel. Then, the KI measurements are done by alternating the fuels twice. The sample fuel's RON is calculated by interpolating the PRF's known RON as a function of their KI readings.

This procedure was followed for the different blends A-x/B-y, and was repeated 3 times on each fuel (to lower the measurement noise due to the repeatability discrepancies). The average results of these 3 series of measurements are presented in the next section.

Octane rating at constant equivalence ratio

The D2699 ASTM RON standard was adapted to suppress the possible impact of the equivalence ratio

variations for the RON measurements. The RON procedure at constant Φ is referenced as RON-Φ and could be summarized as follows:

STEP 1 - CFR engine standardization: same as the standard method's STEP 1.

New STEP 1.2 – Calibration of the knock measure chain: the RON of the fuel blend A-85/B-15 is measured using the standard RON procedure. The calibration obtained (i.e. the spread and meter reading settings) will remain unchanged for the rest of this specific procedure whatever the fuel sample or PRF tested. This is an important difference compared to standard procedure.

STEP 2 - First RON evaluation for the sample fuel: the equivalence ratio is kept constant at Φ=1 (or Φ=0.85). The CR is adjusted so that the standard KI (50) is achieved.

STEP 3 - Selection of PRF: without changing the CR neither the knock measuring chain settings, two PRF blends are selected (PRF1 and PRF2) so that, at constant equivalence ratio, one knocks more (higher KI) and the other less (lower KI) than the sample fuel.

STEP 4 - sample fuel's RON-Φ determination: then, the KI measurements are done by alternating the fuels twice without changing the CR. The sample fuel's RON-Φ is calculated by interpolating the PRF's known RON as a function of their KI readings.

It is relevant to highlight the main differences between the standard ASTM and the constant Φ procedures. The standard procedure operates the engine at the equivalence ratio that maximizes the KI for each sample and PRF whereas the equivalence ratio is kept constant for the constant Φ procedure. Besides, the knock measuring chain is calibrated for each sample in the standard procedure whereas it is calibrated once for all in the constant Φ procedure. Finally, in both methods, the level of KI is standard at 50 and the RON is evaluated by linear interpolation between the sample and the 2 PRFs.

This constant Φ procedure has been followed for the different blends A-x/B-y and the results are presented in the next section (referenced as RON-Φ=1 and RON-Φ=0.85).

SINGLE CYLINDER ENGINE TESTS

The different blends were also tested on a modern spark-ignition direct injection Single Cylinder (SC) engine designed by IFPEN (Figure 5). Its displacement is $351cm^3$ and its compression ratio is 12.5:1 (see Table 6).The fuels are directly injected in the combustion chamber at 200 bar by means of a solenoid centrally mounted injector. The fuel consumption was measured by a MicroMotion CMF010 Coriolis type mass flow meter mounted in the high pressure fuel loop between the rail and the injector. The mass air flow was regulated and measured thanks to a set of sonic nozzles. The equivalence ratio was measured with an UEGO NGK lambda sensor.

Compression Ratio	12,5:1
Displacement	351 cm3
Bore x stroke	72,2 x 85,8 mm
Number of valves	4 per cylinder
Injection	Central direct injection at 200 bar
Cylinder pressure sensor	2 lateral sensors
Fuel mass flow rate measurement	Coriolis flowmeter
Operating conditions	Equivalence ratio constant = 0.85 Fuel mass flow rate constant CA50 set to knock limit (KLSA)

Table 6: Single Cylinder engine specifications.

The cylinder pressure was monitored by two side-mounted sensors: a water-cooled AVL QC34D pressure transducer on one side and a non-water-cooled Kistler 6045A on the other side of the combustion chamber. The pressure signal was acquired every 0,1 CAD and the acquisition process covered 300 engine cycles. The average value of these cycles was used as input data for the calculation of the combustion parameters and the knock intensity.
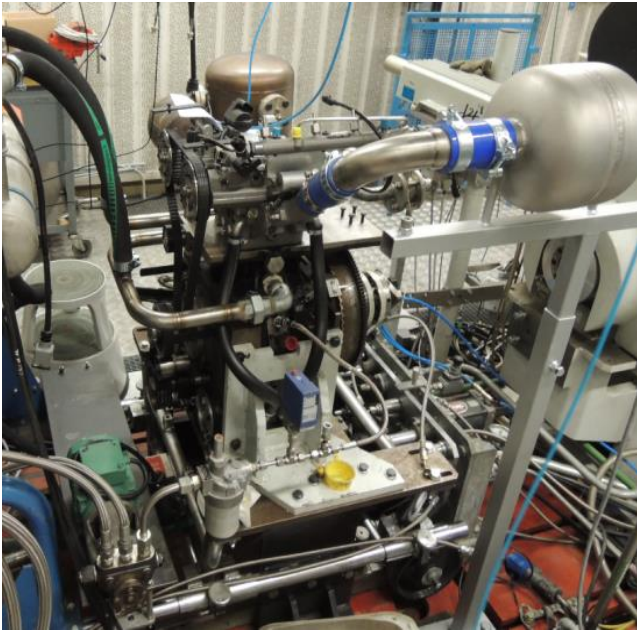
Figure 5: IFPEN Single Cylinder (SC) engine.

The different blends A-x/B-y were tested with the same operating conditions: a constant equivalence ratio of 0.85 and a constant fuel mass flow rate. The spark advance was varied until reaching a repeatable knock limit for the different fuel blends.

RESULTS

In this section are given the results obtained on each experimental device. This section is organized as the previous one: first are given the measurements of ignition delay times, then the octane ratings (standard method and adapted method), and finally the single cylinder engine tests results.

IGNITION DELAY TIMES

Rapid Compression Machine

Figure 6 displays the ignition delay times measured for the fuel blends of A and B in RCM conditions, at a compressed pressure of 20 bar and core gas temperatures T_C of 700 and 850 K, representative respectively of low temperature two-stage ignition and intermediate temperature single-stage ignition. At T_C = 700 K, fuel B displays two-stage ignition with the presence of an intermediate cool flame event related to the so-called Low Temperature branching (further illustrated in Figure 18). Fuel A, however, shows single-stage ignition with an ignition delay which is longer by more than a factor of 10. This is coherent with the amount of aromatics present in the fuel, since aromatics tend to act as radical scavengers through the formation of resonance-stabilized radicals [28]. As fuel B is blended into fuel A, the ignition delay is however hardly modified until the fraction of Fuel A reaches 15%. Similarly, fuels with as much as 10% of Fuel A in B tend to reflect the reactivity of pure B.

At T_C = 850 K, both fuels have more comparable ignition delays of 38 ms for Fuel A and 25 ms for Fuel B, which correlates well with the fact that cyclopentane and most aromatics show very little to no negative temperature coefficient [29]. As Fuel B is blended into Fuel A, the ignition delay decreases slowly up to 70% of Fuel B, where the ignition delay is still 34 ms. At higher Fuel B content, the slope changes and shows greater influence of Fuel B on the ignition delay. The existence of this plateau represents an interesting compromise between resistance to auto-ignition provided by Fuel A, and high LHV provided by Fuel B.
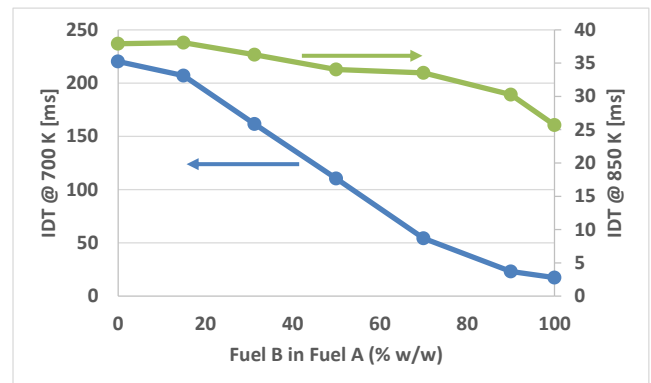

Figure 6: Ignition Delay Times measured at core gas temperatures of 700 K (left axis) and 850 K (right axis), P_{TDC} = 20 bar, Φ = 0.85 in the ULille RCM.

Shock Tube

The ignition delay times were measured on the shock tube for the neat mixtures as well as for the blends. Figure 7 reports the ignition delay times versus the ratio of fuel B added to fuel A, for a reflected shock temperature of 1000 K and a reflected shock pressure of 20 bar. As it can be inferred from the plot, the ignition time of fuel A is equal to 1.198 ms and increases with the addition of fuel B until it reaches the value of 1.77 ms for fuel B. The inhibiting behavior of fuel B when added to fuel A is not surprising given the

nature of both fuels but the slightly non-linear increase of the ignition delay suggests at even at high temperature, cross-reactions are important in the final ignition time.
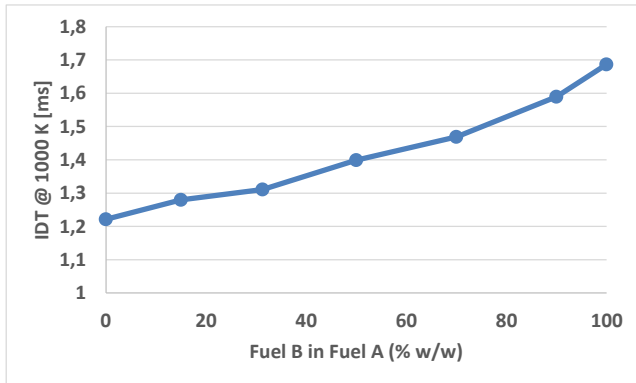

Figure 7: Ignition Delay Times measured at a temperature of 1000 K, P = 20 bar, Φ = 0.85 in the ICARE-CNRS shock tube.

OCTANE RATING

Standard RON, MON and Octane Sensitivity measurements

The first octane rating test campaign was carried out with all the blends A-x/B-y following the standard ASTM RON procedure. The test results for the standard RON in Figure 8 demonstrate a distinctive synergistic behavior between Fuel A and Fuel B. Between 0 and 70% w/w of Fuel B, the blends' RON increase linearly. The maximum standard RON of 104.9 is reached for A-30/B-70 fuel. Above 70% w/w of Fuel B, the standard RON drops dramatically. Consequently, the blends reach standard RON levels well beyond the ones of individual fuels A or B. This synergistic effect between Fuel A and Fuel B allows boosting the level of the blend's standard RON. Whereas RON evolution is atypical, the results of MON reveal a quasi-linear trend for MON vs. Fuel B content.
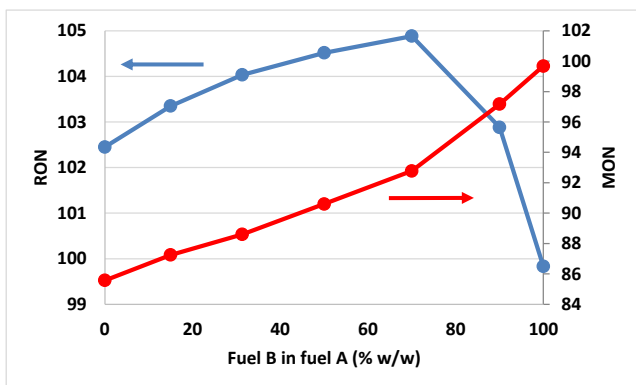
Figure 8: Standard RON and MON measurements.

The consequence of RON and MON trends is the non-linearity of the octane sensitivity shown in Figure 9. The shape of the curve is quasi-linear from 17.3 to 12.2 when fuel B mass content increases from 0 to 70% w/w. Then above 70% w/w, the sensitivity decreases steeply and reaches 0 for pure fuel B.
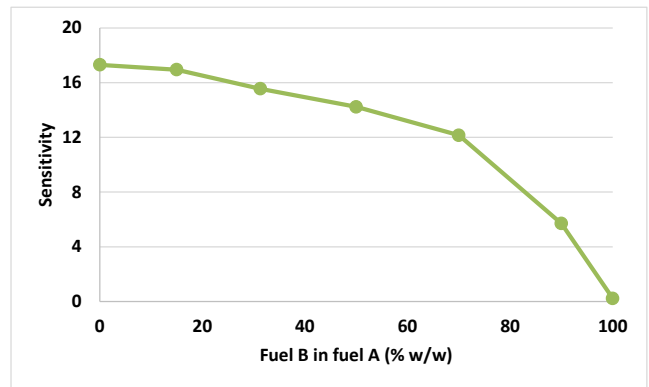

Figure 9: Standard sensitivity measurements.

The UEGO sensor measurements for the standard RON (Figure 10) show that the equivalence ratio varies widely for the different blends. When Fuel B varies from 15 to 70% w/w, the equivalence ratio for standard RON is slightly lean (between 0.98 and 1); otherwise it is rich. The case pure Fuel B reaches the maximum equivalence ratio Φ=1.11. It is relevant to investigate if these variations in equivalence ratio vs. the composition of blends can affect the standard RON measurements. That is why the RON standard procedure was adapted to run RON tests at constant equivalence ratio. It is also important to mention that the equivalence ratio that maximizes the KI for the 2 PRF is richer than the one for the corresponding fuel blend. This will have important consequences on the octane rating at constant equivalence ratio.
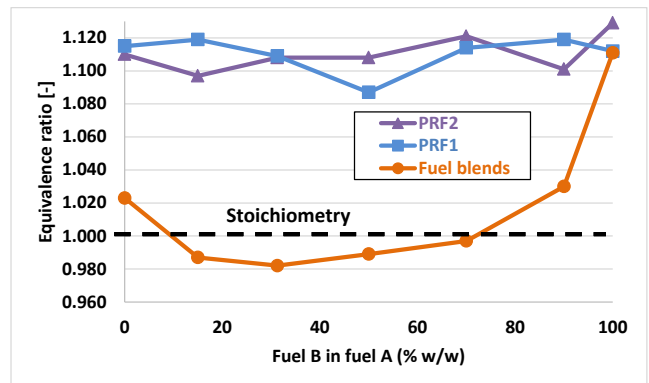

Figure 10: Equivalence ratio measurements during standard RON measurements.

Octane rating at constant equivalence ratio

The second (resp. third) test campaign for the octane rating was carried out at constant equivalence ratios of Φ=1 (resp. Φ=0.85) to suppress the possible impact of equivalence ratio variations on the RON results for the different blends. Figure 11 displays the RON evolutions for the 3 tests campaigns. The most significant result is that the shape of the curves is similar whatever the method used and whatever the level of equivalence ratio. The maximum RON is reached for the same blend A-30/B-70. Thus, it means that the synergistic effect on RON for Fuel A and B is still observed when the equivalence ratio is kept constant. Consequently, this synergy is not due to any "bias" induced by the variable equivalence ratio in standard RON test conditions.

Another observation is that the values of RON-Φ=0.85 are inferior to RON-Φ=1, the latter being also inferior to the standard RON. This result was predictable for the RON-Φ=1. Indeed, the standard RON measurements were done close to the stoichiometry for the different blends (Figure 10). Besides, the standard RON of the PRFs for the standard procedure were measured at equivalence ratios significantly over the stoichiometry (between 1.08 and 1.12 as shown in Figure 10) which corresponds to their equivalence ratio maximizing their KI. Consequently, with the RON-Φ=1 procedure, the KI measured for the different blends didn't change much from the standard RON procedure whereas the KI for the PRF decreased drastically (explained by the fact that stoichiometry is far away from their equivalence ratio maximizing their KI). Thus, to keep the KI levels of the PRF close to the sample level ones, the PRFs' RON for RON-Φ=1 procedure had to be lower than the ones used for the standard procedure in order to increase their KI for these conditions of stoichiometry. These elements explain why the RON-Φ=1 values are lower than the standard RON values.
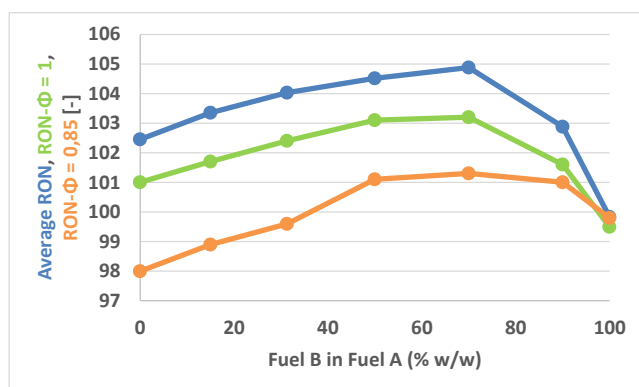
Figure 11: Average standard RON (blue), RON at fixed Φ = 1 (green) and RON at fixed Φ = 0.85 (orange).

The same analysis can be applied to explain the lower values of RON-Φ=0.85 compared to standard RON and RON-Φ=1. For RON-Φ=0.85, the effects described previously are so exacerbated that the minimum RON-Φ=0.85 is obtained for pure Fuel A (even lower than pure Fuel B).

SINGLE CYLINDER ENGINE TESTS

The different fuel blends A-x/B-y were tested at constant equivalence ratio Φ=0.85. The spark advance was adjusted to reach a repeatable knock intensity for each fuel tested.

Figure 12 shows the knock-limited CA50 (crank angle for 50% of Mass Fuel Burnt) and the fuel consumption BSFC results for the different blends. On the one hand, the pure Fuel A has a high RON and octane sensitivity, but a low LHV, and on the other hand, the pure Fuel B has a lower RON and octane sensitivity but a high LHV. According to these statements, it can be expected that the knock resistance of the different blends A-X/B-y should be degraded when Fuel B is progressively added to fuel A. But this is not the trend observed: the knock limited CA50 of the blends remains almost unchanged until 50% w/w of Fuel B incorporated. Even for 70% w/w of Fuel B, the CA50 is

only degraded by 3 CAD. Finally, from 70 to 100% w/w of Fuel B introduced in the blend, the CA50 drastically increases by 10 CAD and the combustion is highly delayed toward the exhaust stroke.
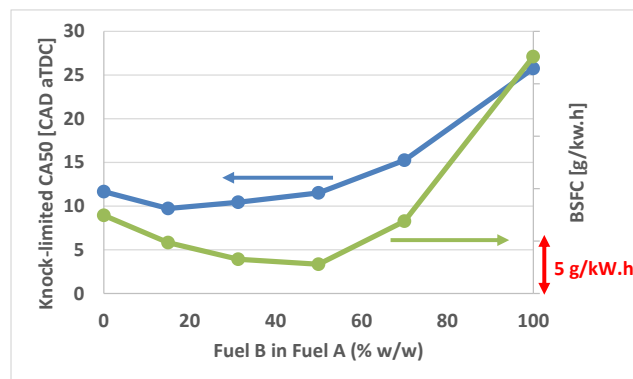

Figure 12: Knock-limited CA50 (left axis) and BSFC (right axis) measured on IFPEN single cylinder engine.

This trend is consistent with the evolution of RON measured on the CFR engine and the synergistic effect between Fuel A and Fuel B discussed above. Thus, it means that it is possible to incorporate large amounts of another component B (with lower RON, lower octane sensitivity and higher LHV) in a Fuel A without degrading the engine efficiency.

As mentioned in the introduction, isooctane (Fuel B), as part of the isoparaffinic family, has one of the highest LHV compared to other hydrocarbons families. This fact, combined to the non-degradation of CA50 when Fuel B is progressively introduced, leads to interesting fuel consumption reductions. From 0 to 50% w/w of Fuel B, the BFSC decreases as the blend's LHV increases at constant CA50. The maximum gain in BSFC is around 5g/kWh for A-50/B-50 compared to pure Fuel A. Moreover, as isooctane (Fuel B) has a lower carbon intensity than Fuel A's (expressed in gCO$_2$/MJ), the maximum BSFC reduction of 5g/kWh for fuel A-50/B-50 leads to nearly 25gCO$_2$/kWh savings (Figure 14).
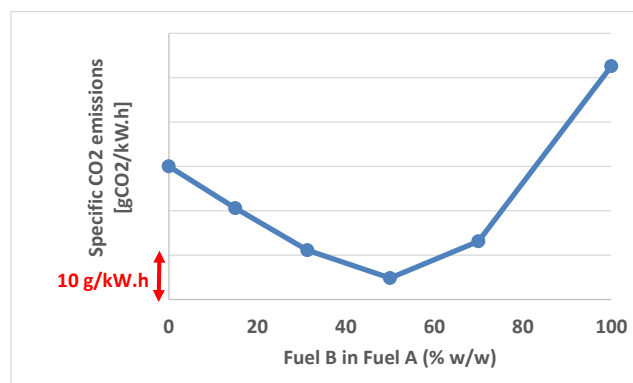

Figure 13: Specific CO$_2$ emissions measured on IFPEN single cylinder engine.

DISCUSSION

This section aims at identifying the compounds responsible for the synergistic effects (in the first paragraph below) and understanding the physical-chemical phenomenon lying behind the

synergies (in the following paragraphs). For the purpose of the latter, several graphs of correlation are presented below. They mainly aim at understanding how the synergy observed on octane numbers can be related to the corresponding ignition delay times, and how the synergy observed on knock-limited CA50 can be related to the corresponding RON, MON, Octane Index and ignition delay times. To facilitate the understanding of the graphs of correlation and their comparisons with each other, all data were normalized between 0 and 1 and are dimensionless; for each graph, a regression line is plotted (dotted line), whose equation and R² is displayed on the graph. Hence, for each graph, the "ideal" correlation would be characterized by an equation $y = x$ and $R^2 = 1$, corresponding to the thin red line (bisector) that appears on each graph.

IDENTIFICATION OF THE COMPOUNDS RESPONSIBLE FOR THE SYNERGISTIC EFFECT ON RON

The RON measurements clearly show a synergistic effect between Fuels A and B, as discussed earlier. As Fuel A is composed of cyclopentane and aromatics, the question is naturally raised whether this synergy with isooctane is due to the presence of cyclopentane or aromatics (or both).

For this purpose, mixtures of cyclopentane and isooctane (A1-x/B-y), as well as mixtures of aromatics and isooctane (A2-x/B-y) were characterized on a CFR engine. As shown in Figure 14, cyclopentane is clearly responsible for the synergistic effect on RON, when the RON of aromatics behaves almost linearly when mixed with isooctane (Figure 15). Interestingly, the addition of isooctane creates a non-linear effect on octane sensitivity in both cases, the non-linearity observed between cyclopentane and isooctane being close to the one observed between Fuels A and B.
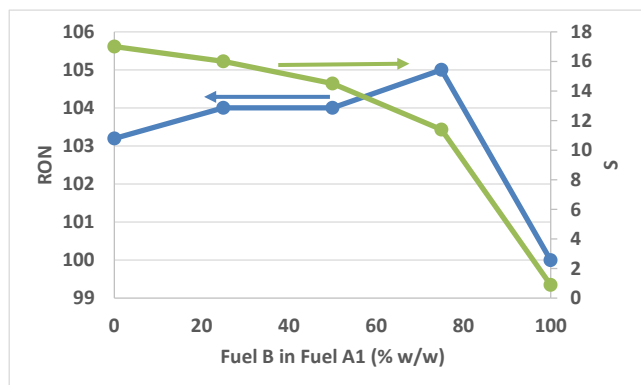

Figure 14: RON (left axis) and octane sensitivity (right axis) of mixtures of cyclopentane (A1) and isooctane (B).
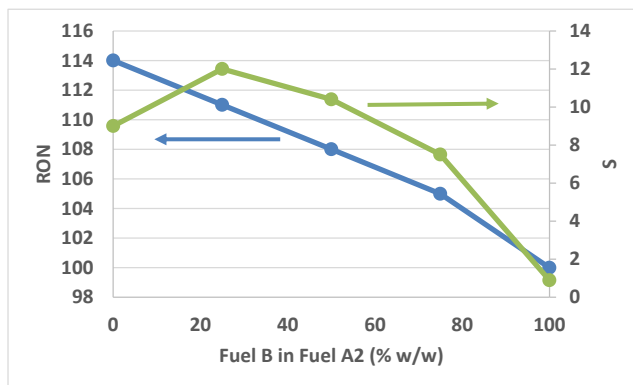

Figure 15: RON (left axis) and octane sensitivity (right axis) of mixtures of aromatics (A2) and isooctane (B).

CORRELATIONS WITH THE IGNITION DELAY TIMES, RON, MON, OCTANE INDEX AND KNOCK-LIMITED CA50

Correlations with the rapid compression machine data

As can be seen in Figure 16, ignition delay times measured on the rapid compression machine do not correlate well with the engine knock-limited CA50. Neither do they correlate with the standard RON (Figure 17) or with the RON at the same equivalence ratio 0.85 (graph not reproduced here).
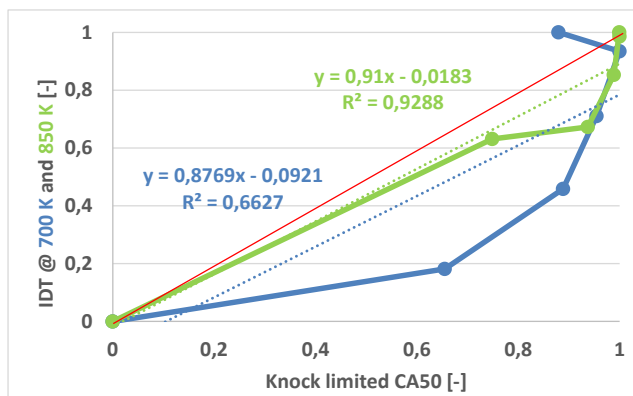

Figure 16: Ignition Delay Times at 700 K (blue) and 850 K (green) vs. knock limited CA50 for the mixtures of Fuels A and B. Normalized data, reduced between 0 and 1.
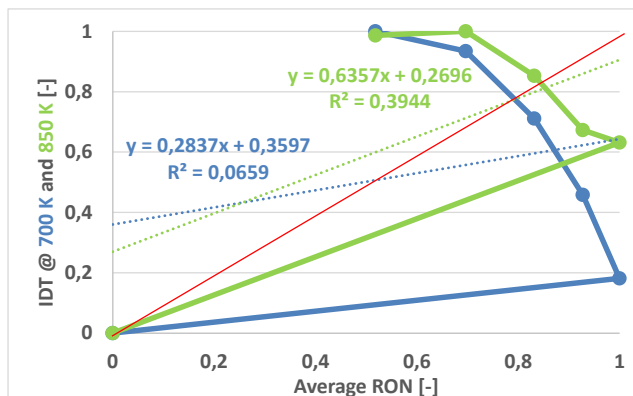

Figure 17: Ignition Delay Times at 700 K (blue) and 850 K (green) vs. average RON for the mixtures of Fuels A and B. Normalized data, reduced between 0 and 1.

Understanding why ignition delay times at 700 K sometimes correlate with RON [12, 30], and

sometimes do not, is challenging and could be key to the reasons for octane synergistic behavior. In the case of this study, this may be due to the two-stage nature of the ignition of Fuel B, and the difference in phenomenology between fuels A and B. As shown in Figure 18 and Figure 19, the cool flame delay (also called 1st stage ignition delay) decreases as more Fuel B is added in the mixture; in parallel, the heat release of the cool flame increases. This increased heat release leads to higher pressure and temperature after the cool flame and has a negative impact on the final ignition delay. At the same time, these more severe conditions are established earlier because of the reduction of the 1st stage ignition delay. It is thus likely that these effects play a major role in the decrease of the ignition delay times at 700 K when Fuel B is added in the mixture, preventing from detecting any synergistic effect with Fuel A (which is expected to be minor compared to this physical-chemical phenomenon). In comparison, as shown by Song et al [31], there is no such heat release of the cool flame with isooctane in a CFR engine during a RON test, allowing to detect and focus on the synergistic effect between Fuels A and B.
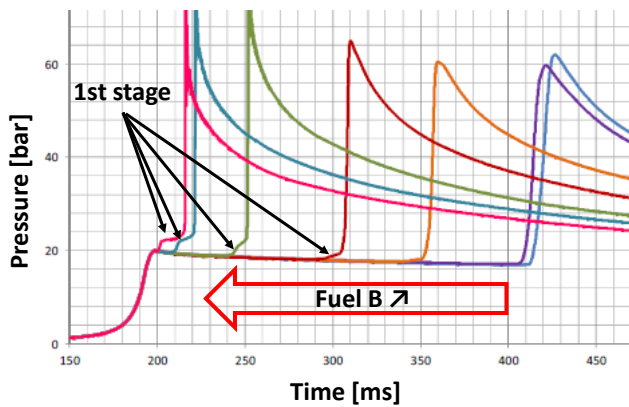

Figure 18: Pressure profiles measured at a core gas temperature of 700 K, P_{TDC} = 20 bar, Φ = 0.85 on the ULille RCM for the mixtures of Fuels A and B.
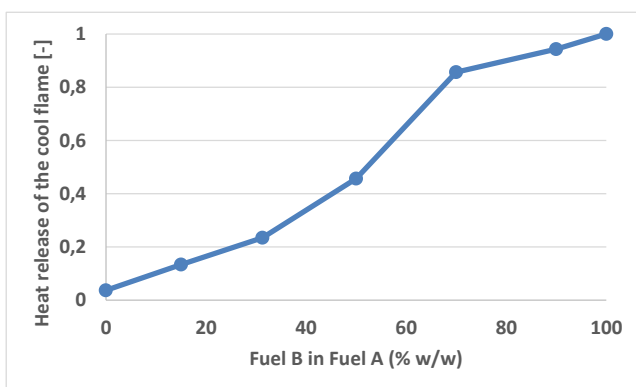

Figure 19: Normalized accumulated chemical heat release induced by the first-stage ignition event at a core temperature of 700 K, P_{TDC} = 20 bar, Φ = 0.85 in the ULille RCM for the mixtures of Fuels A and B.

Correlations with the shock tube data

As shown in Figure 20, the ignition delay times measured on the shock tube at 1000 K do not correlate with the engine knock-limited CA50. In a way, the evolution of these ignition delay times is even

opposed to the one of the knock-limited CA50. This absence of correlation can be explained by the end-gas temperature at knock occurrence which is very different and well below 1000 K, especially in modern turbocharged engines [15].
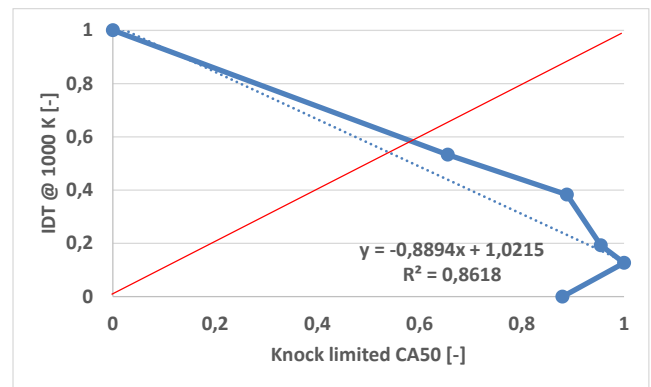

Figure 20: Ignition Delay Times at 1000 K vs. knock limited CA50 for the mixtures of Fuels A and B. Normalized data, reduced between 0 and 1.

On the contrary, the ignition delay times at 1000 K correlate extremely well with the average MON (Figure 21). This correlation can be explained by the high level of temperature of the end-gas in MON test conditions [15].
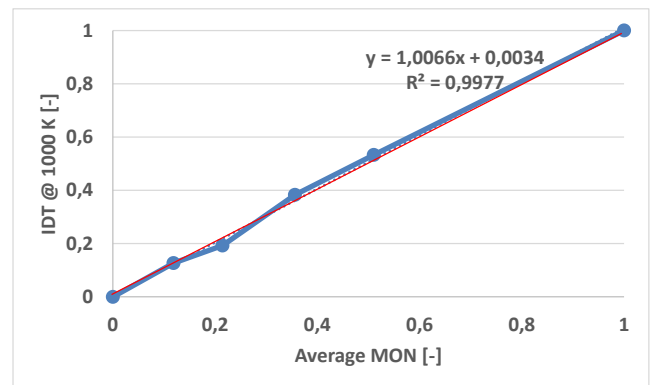

Figure 21: Ignition Delay Times at 1000 K vs. average MON for the mixtures of Fuels A and B. Normalized data, reduced between 0 and 1.

Correlations with the CFR engine data

As shown in Figure 22, the RON measured using the standard ASTM method (blue curve) does not correlate well with the engine knock-limited CA50. Fixing the equivalence ratio on the CFR engine, either at Φ = 1 (green curve) or at Φ = 0.85 (orange curve) does not improve the correlation – it even degrades it. It can thus be concluded that there is no demonstrated interest in modifying the management of the equivalence ratio on a CFR engine to predict engine knock, as surprising as it can be.

Furthermore, Figure 23 shows that the correlation between knock limited CA50 and MON is extremely bad. This is an expected result as it has already been demonstrated by Kalghatgi [16].
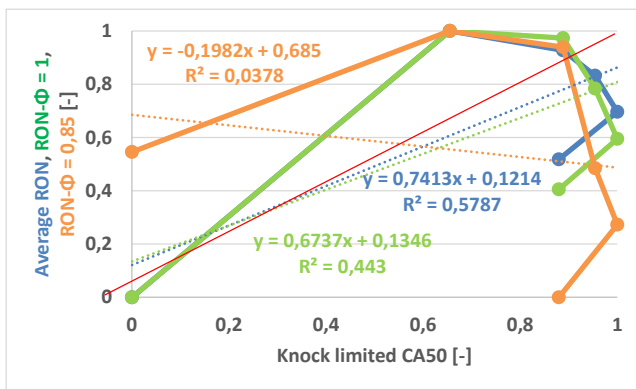
Figure 22: Average RON (blue), RON at fixed Φ = 1 (green) and RON at fixed Φ = 0.85 (orange) vs. knock limited CA50 for the mixtures of Fuels A and B. Normalized data, reduced between 0 and 1.

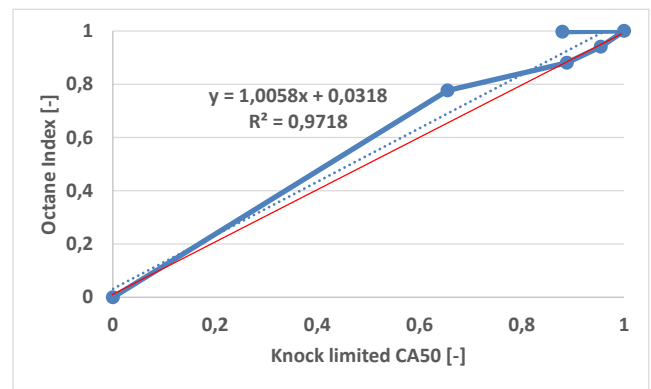*Figure 23: Average MON vs. knock limited CA50 for the mixtures of Fuels A and B. Normalized data, reduced between 0 and 1.*

Then, from the RON, MON and octane sensitivities measured using the standard ASTM methods are computed the corresponding octane index OI, as defined by Kalghatgi [15, 16, 17, 18]:

$$OI = RON – K.S \tag{6}$$

Where K is a parameter depending on the engine and its running conditions (engine speed, load, intake temperature, compression ratio…) which has to be adjusted to correlate with the engine performance (knock-limited CA50 in this study).

Using the octane index, a good correlation is obtained with the knock-limited CA50 (Figure 24) as shown by Kalghatgi. To obtain this correlation, a very negative value of K (K = -2.2) had to be used. Such negative values are seldom found in the literature. The next paragraph will thus focus on this K value and try to explain it.

Figure 24: Octane Index (K = -2.2) vs. knock limited CA50 for the mixtures of Fuels A and B. Normalized data, reduced between 0 and 1.

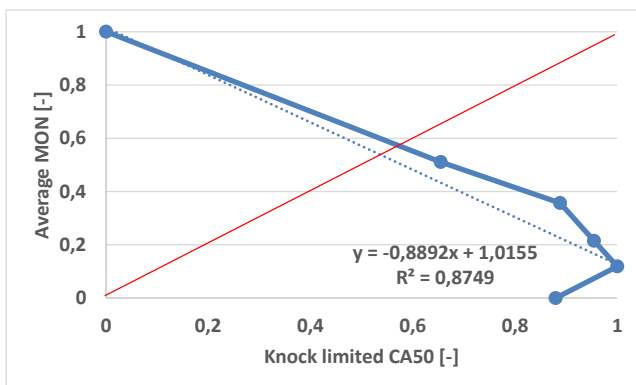## IDENTIFICATION OF A THRESHOLD OF MINIMUM OCTANE SENSITIVITY REQUIRED

To explain this highly negative value of K, two analyses ware carried out:

- In a first analysis, the K value was fitted on the octane index by excluding the fuel having the <u>lowest</u> octane sensitivity (Fuel A-0/ B-100). Hence, in this case, the octane sensitivity ranges between 17.3 and 12.2, which is reasonably high. Under these conditions, K = -0.7, which is considerably less negative than the previous value of -2.2 found for the whole dataset (Figure 25).

- In another analysis, the fuel having the <u>highest</u> octane sensitivity were excluded (Fuel A-100/ B-0). Now, the octane sensitivity lies between 17 and 0, the latter being very low. Under these conditions, the K value approaches minus infinity (K → -∞), which means that the octane index tends to the octane sensitivity (OI → S).
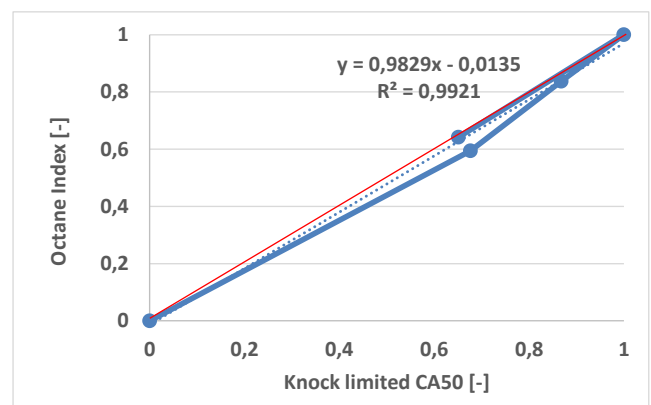

Figure 25: Octane Index (K = -0.7) vs. knock limited CA50 for the mixtures of Fuels A and B (Fuel A-0/ B-100 excluded). Normalized data, reduced between 0 and 1.
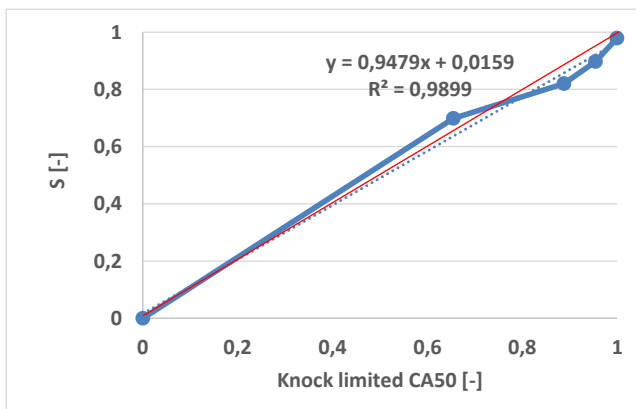
Figure 26: Octane sensitivity (~ Octane Index with K→-∞) vs. knock limited CA50 for the mixtures of Fuels A and B (Fuel A-100/ B-0 excluded). Normalized data, reduced between 0 and 1.

These analyses led on a small dataset show that the K value varies widely depending on the range of octane sensitivity considered: starting from a negative value for the whole range of octane sensitivities, it becomes less negative when the range of octane sensitivities is limited to the highest values, and becomes more negative when the range is displaced towards the lowest octane sensitivities. This statement is then assessed using a larger dataset of 37 fuels (see Figure 27), where RON varies between 92 and 106, MON between 83 and 99 and octane sensitivity ranges between 0 and 17. For this whole dataset, the K value is -1 (Figure 28). If a focus on the fuels having a high octane sensitivity (greater than 14) still gives a K value of -1 (Figure 29), the focus on the low octane sensitivity fuels gives a very negative K of -3 (Figure 30).
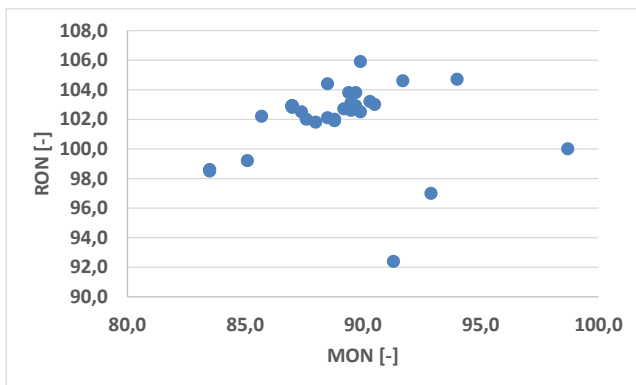

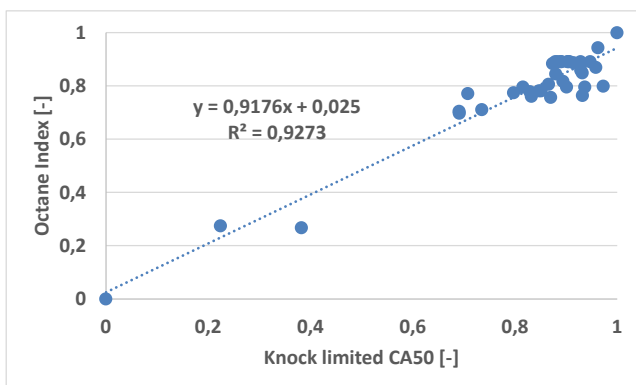*Figure 27: RON and MON characteristics of the 37 fuels evaluated*

Figure 28: Octane Index (K = -1) vs. knock limited CA50 for 37 fuels tested on the same engine with the same
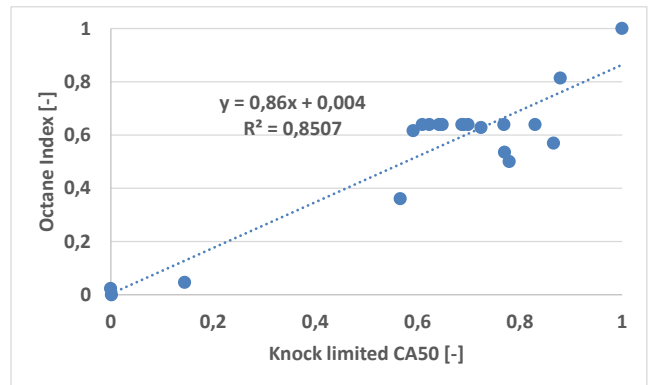
method. Normalized data, reduced between 0 and 1.

Figure 29: Octane Index (K = -1) vs. knock limited CA50 for 20 fuels tested on the same engine with the same method. The 20 fuels are selected from the 37 previous fuels by <u>excluding</u> the fuels having an octane sensitivity <u>lower</u> than 14. Normalized data, reduced between 0 and 1.
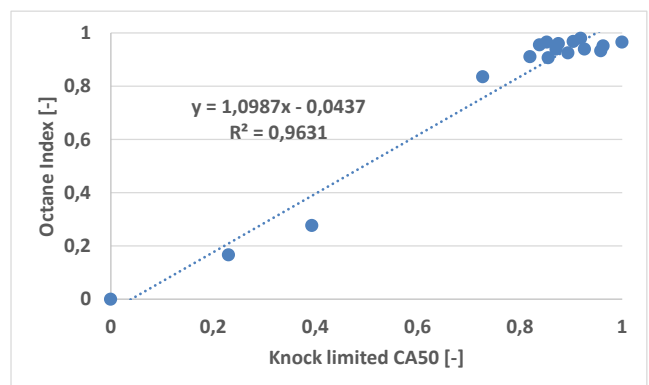

Figure 30: Octane Index (K = -3) vs. knock limited CA50 for 17 fuels tested on the same engine with the same method. The 20 fuels are selected from the 37 previous fuels by <u>excluding</u> the fuels having an octane sensitivity <u>higher</u> than 14. Normalized data, reduced between 0 and 1.

These results lead to an important conclusion: if the K value is very negative for the lower sensitivity fuels (S < 14), it means that octane sensitivity is the most important parameter to increase to improve the knock resistance of fuels whose octane sensitivity is below a certain threshold. Once this threshold is reached, the K value becomes less negative, which means that RON and octane sensitivity are more or less equally important to increase the fuels performance.

	Fuels A and B mixtures	All 37 fuels
Full dataset	K = -2.2	K = -1
High Sensitivity fuels	K = -0.7	K = -1
Low Sensitivity fuels	K → -∞	K = -3

Table 7: K values calculated for the mixtures of Fuels A and B (left) and all 37 fuels (right). 1st line: for the full dataset; 2nd line: for a selection of the high-S fuels; 3rd line: for a selection of the low-S fuels. It is remarkable that isolating the low-S fuels always leads to more negative K values.

CONCLUSIONS

The following conclusions can be drawn out of the findings of this study:

- There is a synergistic effect between cyclopentane and isooctane allowing the mixtures of these compounds to reach RON values well beyond the ones of their individual compounds. A similar non-linearity is observed on their octane sensitivity, although the synergy is not as high. Similar synergistic effects had been demonstrated in the literature earlier with other compounds: between diisobutylene and isooctane [10] and between ethanol and isooctane [11]. Isooctane is thus often implied in synergistic effects on RON and octane sensitivity.

- As long as the K value of the engine is negative (which is mostly the case in modern turbocharged engines), these synergistic effects allow maintaining the octane index at a high value when incorporating high rates of isooctane. Hence, these mixtures based on a relatively high rate of isooctane with cyclopentane keep a good resistance to knock despite the isooctane's bad knock resistance when considered individually.

- Isooctane (and more generally speaking isoparaffins) having among the highest lower heating value (expressed in MJ/kg) and among the lowest carbon intensities (expressed in gCO_2/MJ) compared to the other fossil-based hydrocarbons families (especially compared to aromatics), its synergistic effect with cyclopentane on knock resistance leads to lower specific fuel consumptions (BSFC, in g/kW.h) and lower specific CO_2 emissions (in gCO_2/kW.h). This paves the way to new formulation opportunities for highly efficient gasolines, containing high ratios of isoparaffins, despite the poor knock resistance of numerous isoparaffins (including isooctane) when individually considered.

- The study did not manage to find any correlation between RON and the ignition delay times. While no correlation was expected between RON and the ignition delay times at 850 K and 1000 K because they are not in the appropriate range of temperature, a correlation could have been expected with the ignition delay times at 700 K. However, the study shows that when incorporating isooctane in cyclopentane, the first-stage ignition delay decreases and the cool flame heat release increases, resulting in shortened ignition delay times, and preventing from observing the synergistic effect observed on RON. Therefore, the study did not manage to explain properly the synergistic effect between isooctane and cyclopentane. More understanding is still needed to be able to address this issue.

- MON correlates very well with ignition delay times at 1000 K. This can be explained by the appropriate range of temperature used in the shock tube in these experiments, and the absence of cool flame at this range of temperature.

- The synergistic effect on RON is still observed when the equivalence ratio in the CFR engine is kept constant ($\Phi = 1$ or $\Phi = 0.85$). Hence, this synergy is "real" and not due to a bias induced by the variable equivalence ratio in RON test conditions. However, keeping the equivalence ratio constant on the CFR engine did not improve the prediction of fuels knock resistance in a real engine (it is even the opposite). Therefore the study sees no interest in modifying the standard RON test procedure for engine knock prediction.

- Among all the experimental device and methods tested (rapid compression machine at 700 K and 850 K, shock tube at 1000 K, standard or adapted CFR tests), the study concludes that prediction on fuels engine-knock resistance can better be obtained from the standard RON and MON measurements, which allow to calculate their octane index (OI = RON – K.S). As far as the shock tube is concerned, the extension to lower temperature (and hence longer ignition delay times) would be necessary to match engine thermal conditions, which can be achieved through higher pressure conditions in the shock tube.

- The K value of the octane index is very negative for the fuels having a low sensitivity, and is less negative for the fuels having a higher sensitivity. Therefore, increasing the octane sensitivity is crucial to improve the knock resistance of low-sensitivity fuels, while RON and octane sensitivity are more or less equally important to the performance of the high-sensitivity ones.

REFERENCES

1. ICCT, "The European Commission regulatory proposal for post-2020 CO2 targets for cars and vans: A summary and evaluation", Jan 2018, https://www.theicct.org/sites/default/files/publicati

ons/ICCT_EU-CO2-proposal_briefing_20180109.pdf.

2. Johnson, T. and Joshi, A., "Review of Vehicle Engine Efficiency and Emissions," SAE Technical Paper 2018-01-0329, 2018, doi: 10.4271/2018-01-0329.

3. Prakash, A., Redmann, J.-H., Giles, K., Cracknell, R. et al., "Octane Response of a Highly Boosted Direct Injection Spark Ignition Engine at Different Compression Ratios," SAE Technical Paper 2018-01-0269, 2018, doi:10.4271/2018-01-0269.

4. Heywood, J., "Internal combustion engine", McGraw Hill Book Co., 1988, ISBN:0-07-028637-X.

5. 2018 Formula One Technical Regulations

6. https://www.acea.be/statistics/tag/category/cubic-capacity-average-power, accessed 09/18/2018

7. Knop, V., Loos, M., Pera, C., and Jeuland, N., "A linear-by-mole blending rule for octane numbers of n-heptane/iso-octane/toluene mixtures", Fuel, Vol. 115, pp 666-673, Jan 2014, doi: 10.1016/j.fuel.2013.07.093.

8. Rankovic, N., Bourhis, G., Loos, M., and Dauphin, R., "Understanding octane number evolution for enabling alternative low RON refinery streams and octane boosters as transportation fuels", Fuel, Vol. 150, pp 41-47, June 2015, doi: 10.1016/j.fuel.2015.02.005.

9. Morgan, N., Smallbone, A., Bhave, A., Kraft, M., Cracknell, R., and Kalghatgi, G., "Mapping surrogate gasoline compositions into RON/MON space", Combustion and Flame, Vol. 157 (6), pp 1122-1131, June 2010, doi: 10.1016/j.combustflame.2010.02.003.

10. Bradow, R., and Alperstein, M., "Analytical investigations of isooctane and diisobutylene slow combustion in an Otto-cycle engine", Combustion and Flame, vol. 11, pp. 26-34, 1967, doi: 10.1016/0010-2180(67)90006-5.

11. Foong, T.M., Morganti, K.J., Brear, M.J., da Silva, G., Yang, Y., and Dryer, F.L., "The octane numbers of ethanol blended with gasoline and its surrogates", Fuel, Vol. 115, pp. 727-739, Jan 2014, doi: 10.1016/j.fuel.2013.07.105.

12. Jarrosson, F., Fenard, Y., Vanhove, G., and Dauphin, R. "Gasoline and Combustion: Relationship between Molecular Structure and Performance," SAE Technical Paper 2018-01-0906, 2018, doi: 10.4271/2018-01-0906.

13. Barrufet, M.A., "Reservoir Fluids, Petroleum Engineering, Pure components Data," http://www.pe.tamu.edu/barrufet/public_html/PETE310/, accessed 07/13/2016.

14. Boot, M., Tian, M., Hensen, E. and Sarathy, M., "Impact of fuel molecular structure on auto-ignition behavior – Design rules for future high performance gasolines", Progress in Energy and Combustion Science, Vol. 60, pp 1-25, 2017, doi: 10.1016/j.pecs.2016.12.001

15. Cracknell, R., Warnecke, W., Redmann, J.-H., and Goh, T.K., "Octane Requirements of Modern Downsized Boosted Gasoline Engines", MTZ, Vol. 76, pp 4-7, 2015.

16. Kalghatgi, G.T., "Fuel Anti-Knock Quality- Part II. Vehicle Studies - How Relevant is Motor Octane Number (MON) in Modern Engines?", SAE Technical Paper 2001-01-3585, 2001, doi: 10.4271/2001-01-3585

17. Kalghatgi, G., Nakata, K., and Mogi, K., "Octane Appetite Studies in Direct Injection Spark Ignition (DISI) Engines," SAE Technical Paper 2005-01-0244, 2005, doi: 10.4271/2005-01-0244

18. Kalghatgi, G.T., "Fuel Anti-Knock Quality – Part I. Engine Studies", SAE Technical Paper 2001-01-3584, 2001, doi: 10.4271/2001-01-3584.

19. Lu, Z., Yang, Y., and Brear, M.J., "Oxidation of PRFs and ethanol/iso-octane mixtures in a flow reactor and the implication for their octane blending", Proceedings of the Combustion Institute, Aug 2018, doi: 10.1016/j.proci.2018.05.134.

20. Somers, K.P., Cracknell, R.F., Curran, H.J., "A chemical kinetic interpretation of the octane appetite of modern gasoline engines", Proceedings of the Combustion Institute, June 2018, doi: 10.1016/j.proci.2018.05.123

21. Yu, Y., Vanhove, G., Griffiths, J.F., De Ferrières, S., and Pauwels, J.-F, "Influence of EGR and Syngas Components on the Autoignition of Natural Gas in a Rapid Compression Machine: A Detailed Experimental Study", Energy Fuels, 27 (7), pp 3988-3996, June 2013, doi: 10.1021/ef400336x.

22. Fenard, Y., Boumehdi M., and Vanhove, G., "Experimental and Kinetic Modeling Study of 2-Methyltetrahydrofuran Oxidation under Engine-Relevant Conditions," Combustion and Flame, vol. 178, pp 168-181, Apr 2017, doi:10.1016/j.combustflame.2017.01.008.

23. Goldsborough, S.S., Fridlyand, A., Santner, J., Rockstroh, T., and Jespersen, M.C., "Heat release analysis for rapid compression machines: Challenges and opportunities", Proceedings of the Combustion Institute, Aug 2018, doi: 10.1016/j.proci.2018.05.128

24. Comandini, A., Pengloan, G., Abid, S., and Chaumeix, N., "Experimental and modeling study of styrene oxidation in spherical reactor and shock tube", Combustion and Flame, vol. 173, pp. 425-440, Nov 2016, doi: 10.1016/j.combustflame.2016.08.026

25. Comandini, A., Dubois, T., Abid, S., and Chaumeix, N., "Comparative study on cyclohexane and decalin oxidation", Energy Fuels, 2014, 28 (1), pp 714–724, doi: 10.1021/ef402046n

26. Standard Test Method for Research Octane Number of Spark- Ignition Engine Fuel, ASTM International D2699.

27. Standard Test Method for Motor Octane Number of Spark-Ignition Engine Fuel, ASTM International D2700.

28. Vanhove, G., Petit, G., and Minetti, R., "Experimental study of the kinetic interactions in the low-temperature autoignition of hydrocarbon binary mixtures and a surrogate fuel", Combustion

and Flame, vol. 145, issue 3, pp 521-532, May 2006, doi: 10.1016/j.combustflame.2006.01.001.

29. Roubaud, A., Minetti, R., and Sochet, L.R., "Oxidation and combustion of low alkylbenzenes at high pressure: comparative reactivity and auto-ignition", Combustion and Flame, vol. 121, issue 3, pp 535-541, March 2000, doi: 10.1016/S0010-2180(99)00169-8.

30. Singh, E., Badra, J., Mehl, M. and Sarathy, M., "Chemical Kinetic Insights into the Octane Number and Octane Sensitivity of Gasoline Surrogate Mixtures", Energy & Fuels, Vol. 31, 1945–1960, 2017, doi: 10.1021/acs.energyfuels.6b02659.

31. Song, H. and Song, H., "Knock Prediction of Two-Stage Ignition Fuels with Modified Livengood-Wu Integration Model by Cool Flame Elimination Method," SAE Technical Paper 2016-01-2294, 2016, doi:10.4271/2016-01-2294.

CONTACT

Roland Dauphin: roland.dauphin@total.com

DEFINITIONS, ACRONYMS, ABBREVIATIONS

AFR   Air/Fuel ratio in stoichiometric conditions

BMEP   Brake Mean Effective Pressure

BSFC   Brake Specific Fuel Consumption

BSCO$_2$ Brake Specific CO_2 emissions

CA50   Crank Angle of 50% burnt mass fraction

CAD   Crank Angle Degree

CFR   "Cooperative Fuels Research"

CI   Carbon Intensity

CR   Compression Ratio

GDI   Gasoline Direct Injection

HRR   Heat Release Rate

IDT   Ignition Delay Time

KLSA   Knock Limited Spark Advance

KI   Knock Intensity

LHV   Lower Heating Value

MON   Motor Octane Number

OI   Octane Index

ON   Octane Number

PRF   Primary Reference Fuel

RCM   Rapid Compression Machine

RON   Research Octane Number

RON-Φ   RON using fixed equivalence ratio

S   Octane Sensitivity

SI   Spark Ignition

SC   Single Cylinder

ST   Shock Tube

TDC   Top Dead Center

UEGO   Universal Exhaust-Gas Oxygen

η$_{comb}$ Combustion efficiency

η$_{cycle}$ Cycle efficiency

η$_{eff}$ Effective efficiency

η$_{mech}$ Mechanical efficiency

η$_{th.th}$ Theoretical thermodynamic efficiency

γ   Specific heat ratio

ε   Compression ratio

Φ   Equivalence ratio

τ   Ignition delay time